GAS GIANT PLANETS

Loss of a satellite could explain Saturn's obliquity and young rings

Jack Wisdom[1]*, Rola Dbouk[1], Burkhard Militzer[2,3], William B. Hubbard[4], Francis Nimmo[5], Brynna G. Downey[5], Richard G. French[6]

The origin of Saturn's ~26.7° obliquity and ~100-million-year-old rings is unknown. The observed rapid outward migration of Saturn's largest satellite, Titan, could have raised Saturn's obliquity through a spin-orbit precession resonance with Neptune. We use Cassini data to refine estimates of Saturn's moment of inertia, finding that it is just outside the range required for the resonance. We propose that Saturn previously had an additional satellite, which we name Chrysalis, that caused Saturn's obliquity to increase through the Neptune resonance. Destabilization of Chrysalis's orbit ~100 million years ago can then explain the proximity of the system to the resonance and the formation of the rings through a grazing encounter with Saturn.

Saturn's obliquity, the angle between its equator and the plane of its orbit around the Sun, is too large to have arisen during Saturn's formation from a protoplanetary disk or from a large impact (*1*). Saturn's rings appear to be only ~100 million years (Myr) old, based on the estimated strength of satellite ring torques (*2*) and the estimated rate of darkening of the ice-rich material (*3*, *4*). However, the lack of a suitable mechanism to explain such young rings has led some to question the young age (*5*).

The precession frequency of Saturn's spin axis (the rate at which the axis rotates about the vertical) is close to the precession frequency of Neptune's orbit (*6*). This raises the possibility that the obliquity resulted from a resonance between these two frequencies. Resonances between the precession of the spin axis of a body and the precession of its orbit occur elsewhere in the Solar System. The spin axis of the Moon and the orbit of the Moon precess at the same rate (*7*, *8*). Spin-orbit precession resonances also arise if the precession frequency of a spin axis is close to a frequency component in the precession of its orbit. Mars has a chaotic obliquity due to a resonance between the precession of its spin axis and a chaotically varying component in its orbit precession associated with the precession of Venus (*9*, *10*). The obliquity of the Moon, locked in the precession resonance, depends on the rate of mutual precession of the orbit and spin axis. The Moon's obliquity was different in the past because the rate of orbit precession depends on the distance to Earth and the Moon is tidally evolving outward from Earth. There were times when the obliquity of the Moon was large (*11*).

If the large obliquity of Saturn is the result of a spin-orbit resonance between the precession of Saturn's spin axis and the precession of the orbit of Neptune, how would this have come about? One proposal is that the precession frequency of Neptune's orbit could have changed as the distribution of protoplanetary mass changed during planet formation (*1*). An alternative proposal relies upon the observed rapid migration of Saturn's largest satellite, Titan (*12*–*14*). The precession frequency of Saturn is modified by the presence of its satellites, which are locked to orbit in the equatorial plane of Saturn. Because of this lock, the Sun's gravitational pull on the satellites contributes to the torque that precesses Saturn. The precession of Saturn is dominated by these solar torques on Titan, which are proportional to the square of the distance of Titan from Saturn (*11*), so as Titan migrates outward, the precession frequency increases. This could have caused the precession frequency of the Saturn system to become resonant with the precession of Neptune (*12*). We define a resonance angle σ to be the longitude of Saturn's equator minus the longitude of the descending node of Neptune's orbit (*10*). While in the Neptune resonance, this angle oscillates about zero. If the migration of Titan was slow, compared with the period of oscillation in the precession resonance, the obliquity of Saturn could have risen as Titan migrated (*13*).

Both of these scenarios require the moment of inertia of Saturn to be in a certain range and predict that the system is currently in this spin-orbit precession resonance. Previous determinations of the moment of inertia had too high an uncertainty to draw definitive conclusions (*1*, *12*).

Moment of inertia of Saturn

The exterior gravity field of Saturn, as determined using the Cassini spacecraft (*4*), provides tight constraints on models of the planet's interior structure. We constructed interior models using four different sets of assumptions. For a range of rotation periods, the corresponding moments of inertia are shown in Fig. 1 in terms of the normalized angular momentum: the product of the moment of inertia and the rotation rate,

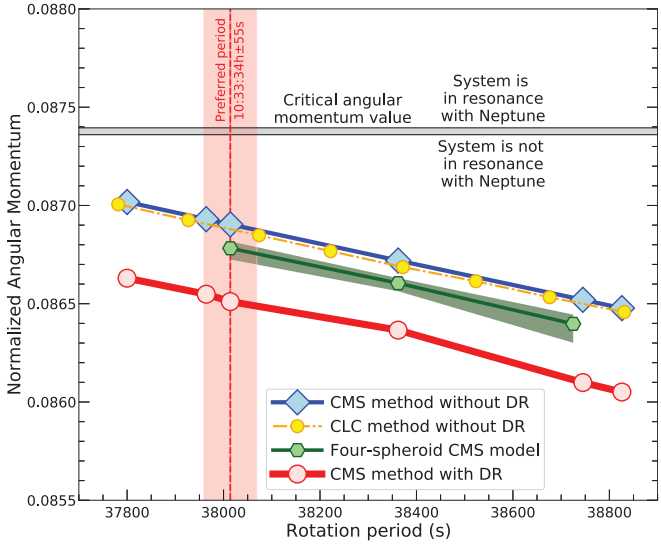

Fig. 1. Saturn's normalized angular momentum as a function of rotation period. The red curve and circles represent results for models using physical equations of state with differential rotation (DR), matched to the even gravitational moments up to J_{12}. The other three models assume uniform rotation and only match J_2, J_4, and J_6. The results of the consistent level curve method (yellow dash-dotted curve and circles) and the CMS method (blue curve and diamonds) are consistent with each other and close to the more approximate four-spheroid CMS results (green curve and hexagons). The green-shaded region indicates the range of results for an ensemble of four-spheroid CMS models that each match the gravitational moments. The vertical red line and band indicate the rotation period (and uncertainty) estimated from the measured flattening of Saturn. The horizontal gray band (between 0.087360 and 0.087399) indicates the critical value to be in the precession resonance. All models fall below the critical value, so the system is near, but not in, the spin-orbit precession resonance. Numeric values are listed in table S1.

[1]Department of Earth, Atmospheric, and Planetary Sciences, Massachusetts Institute of Technology, Cambridge, MA 02139, USA. [2]Department of Astronomy, University of California, Berkeley, CA 94720, USA. [3]Department of Earth and Planetary Science, University of California, Berkeley, CA 94720, USA. [4]Lunar and Planetary Laboratory, University of Arizona, Tucson, AZ 85721-0092, USA. [5]Department of Earth and Planetary Sciences, University of California, Santa Cruz, CA 95064, USA. [6]Department of Astronomy, Wellesley College, Wellesley, MA 02481, USA.
*Corresponding author. Email: wisdom@mit.edu

normalized by $MR_e^2\sqrt{GM/R_e^3}$, where G is the gravitational constant, M is the mass of Saturn, and R_e is its fiducial equatorial radius, taken to be 60,268 km (*15*).

We combine an equation of state for hydrogen-helium mixtures (*16*) with assumptions about Saturn's interior composition. We assume that the interior of Saturn is differentially rotating on cylinders, chosen to match cloud tracking observations. We use the concentric Maclaurin spheroid (CMS) method (*17*, *18*) to construct models that match (fig. S1) the gravitational moments from J_2 to J_{12} (*4*). The Js are dimensionless coefficients in the expansion of the exterior gravity field. Normalized angular momentum values are shown in Fig. 1 and listed in table S1.

To estimate how much the computed moment of inertia depends on the assumptions, we used three additional approaches to construct models of the interior of Saturn. These models only match the gravitational moments J_2, J_4, and J_6 without invoking differential rotation.

The first approach uses the consistent level curve method (*19*), with polynomial equations of state that relate pressure and density. The order of the polynomial is increased until the values of J_2 to J_6 can be reproduced. The second approach uses the CMS method as before but introduces a single discontinuity in the density to match J_2 to J_6 without differential rotation. The third method introduces more flexibility by representing Saturn's interior with four constant-density spheroids. Their densities and thicknesses are adjusted until the observed moments up to J_6 can be matched with CMS calculations. The resulting spread of model predictions is indicated in Fig. 1 and fig. S2. Results for a larger number of spheroids are shown in fig. S3. We find consistent results from all models that match J_2, J_4, and J_6 while assuming uniform rotation. The angular momentum depends only on the assumed rotation rate and the observed gravitational moments.

Models that assume uniform rotation do not match the high-order gravitational moments (J_8 to J_{12}). The observed large magnitudes of the high-order moments are indicative of differential rotation (*4*, *20*). However, the inclusion of differential rotation lowers the implied angular momentum by only ~0.5% (Fig. 1).

The resulting moments of inertia are in close agreement with one another, indicating that they are tightly constrained by the gravitational moments and insensitive to the assumed composition and equation of state. The values of J_2 and J_4 alone provide sufficient constraints on the planet's angular momentum to show that Saturn is slightly out of resonance with Neptune (see supplementary text). Models without differential rotation provide an upper bound on the angular momentum, whereas including differential rotation (to match the higher-order gravitational moments) reduces the angular momentum slightly (Fig. 1 and fig. S4) (see supplementary text).

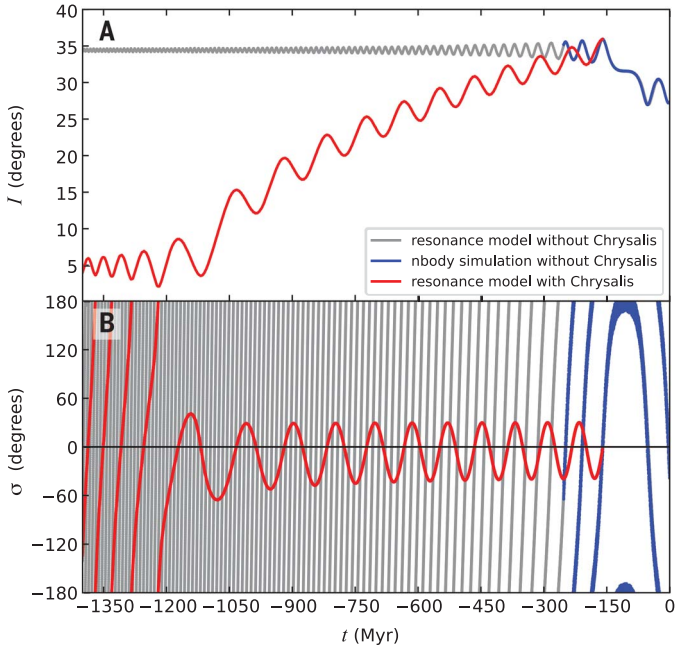

Fig. 2. Saturn evolution. (**A** and **B**) Obliquity of Saturn I (A), and the resonance angle σ (B), as a function of time t. The obliquity is with respect to the invariable plane, the plane perpendicular to the total angular momentum of the Solar System. The blue curve is a full numerical simulation, with da_{Titan}/dt = 13.75 cm year^{-1}, where a_{Titan} is the semimajor axis of Titan. The gray curve is the resonance model. At recent times, it coincides with the blue curve. The red curve is the resonance model with Chrysalis. Chrysalis has an instability around 160 Myr before present and is removed from the system.

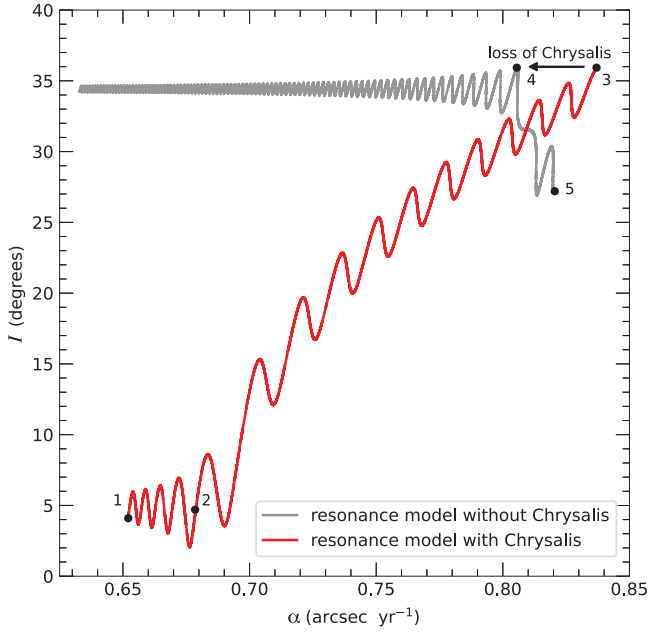

Fig. 3. Evolution as a function of precession constant. The system starts outside the Neptune resonance at point 1. As Titan migrates, the precession constant increases, and the system enters the resonance at point 2. With continued evolution, the obliquity of Saturn increases. At point 3, Chrysalis experiences an instability and has a close encounter with Saturn, forming the rings. The precession constant suddenly decreases to point 4. Further evolution, without Chrysalis, carries the system to point 5, at the present.

Numerical integrations of the satellite system

We used numerical integration to investigate the dynamical evolution of the Saturn satellite system. These integrations include Saturn, modeled as a rigid body; the gravitational moments of Saturn from J_2 to J_6; the major satellites of Saturn from Mimas to Iapetus; the Sun; and the other three outer planets. The system is fully coupled: The gravitational moments affect the motion of the satellites as well as the rotation of Saturn. Some of our integrations included tidal evolution, specified by the rate of change of Titan's semimajor axis; for simplicity, we ignore the tidal evolution of the other satellites (*21*).

We used direct numerical integration to determine the range of moments of inertia of Saturn for which the system is in the spin-orbit precession resonance. Numerical integration avoids the need to analytically estimate a host of small effects (*21*). We refer to the lower bound of this range as the critical value. We performed a series of forward and backward

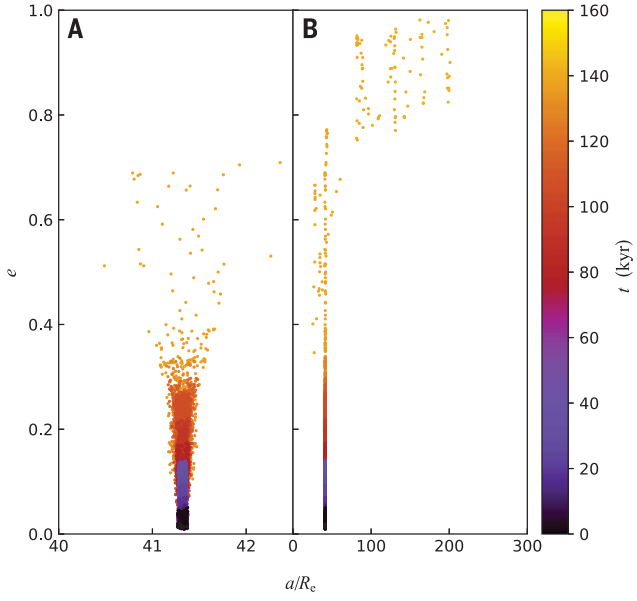

Fig. 4. Eccentricity of Chrysalis as a function of its semimajor axis, in an example simulation. (**A** and **B**) The early evolution in the chaotic zone is visible in (A). In (B), the chaotic phase shown in (A) appears as a spike on the left; the semimajor axis (*a*) and eccentricity (*e*) increase because of scattering encounters with Titan and Iapetus. Time, in thousand years (kyr), is indicated by the color bar. The trajectory is sampled every 500 years.

50-million-year integrations to determine the critical moment of inertia. These integrations did not include tidal friction and excluded the tiny satellite Hyperion. The results are also shown in Fig. 1, in terms of the normalized angular momentum. We find that the system is outside, but close to, the resonance region for all model assumptions and rotation periods. If we adopt a rotation period of 10:33:34 hours, derived by matching Saturn's flattening (*15*, *18*), the predicted angular momenta are between 0.5 and 1.0% below the critical value.

The critical angular momentum to be in resonance corresponds to a dimensionless polar moment of inertia of 0.2201. The estimated value, with differential rotation, for a rotation period of 10:33:34 hours is $0.2182^{+0.0006}_{-0.0003}$, which is about 1% below the critical value. Previous work (*12*), though more approximate, found that for Saturn to have had an initial obliquity less than 10°, the moment of inertia must be in the range 0.224 to 0.237, and for Saturn to be oscillating in the resonance, it must be between 0.22 and 0.24, a 10% range.

Small changes in the system parameters can make large changes in the rate of precession. For example, changing the semimajor axis of Saturn by only 5% changes the rate of precession by 15% (Eq. 1). Similarly, making small changes in the mass or position of Uranus or Neptune can also make large changes in the precession frequency of Neptune. So, the system being only 1.0% away from the resonance suggests that the Neptune resonance has played a role in the recent history of the Saturn system.

The rapid migration of Titan rules out scenarios that depend on the Neptune resonance in the early Solar System (*12*). If the Neptune resonance played a role in the development of the obliquity of Saturn, it rules out other proposed early Solar System explanations (*22*, *23*). We propose that the obliquity of Saturn arose because the system was previously trapped in the Neptune resonance as Titan migrated outward but escaped from the resonance recently enough to still be near the resonance.

Resonance model

We construct a simple model that captures many aspects of the dynamics of the spin-orbit precession resonance with Neptune (*21*). This model can be used to interpret the results of the full numerical simulations.

A parameter in this model is the precession constant. Averaging over the orbital time scale, an oblate planet with satellites orbiting the Sun in a fixed circular orbit has a rate of regression of the spin axis of $\alpha\cos(\epsilon)$, where α is the precession constant and ϵ is the obliquity of the spin axis to the fixed orbit normal. The precession constant is (*11*, *13*)

$$\alpha = \frac{3}{2} n \frac{n}{\omega} \frac{J_2 + q}{\lambda + l} \tag{1}$$

where n is the orbital frequency; ω is the rotation rate; J_2 is the second gravitational moment; $\lambda = C/(MR_e^2)$ is the dimensionless polar moment of inertia, where C is the moment of inertia; and

$$q = \frac{1}{2}\sum_j \frac{m_j}{M}\frac{a_j^2}{R_e^2}\frac{\sin\left[2\left(\epsilon - i_j^L\right)\right]}{\sin(2\epsilon)}$$

$$l = \sum_j \frac{m_j}{M}\frac{a_j^2}{R_e^2}\frac{n_j}{\omega}\frac{\sin\left(\epsilon - i_j^L\right)}{\sin(\epsilon)} \tag{2}$$

The sum is over all the satellites, indexed by j; m_j is the mass of the satellite; a_j is the semimajor axis of the satellite; and n_j is its orbital frequency. The angle i_j^L is the inclination of the Laplace plane to the planetary equator (*24*); the normal to the Laplace plane is the direction about which the normal to the satellite orbit precesses. For a close satellite, the Laplace plane coincides with the planetary equator plane, whereas for a distant satellite, it coincides with the plane of the orbit of the planet about the Sun. The magnitude of i_j^L depends on the planetary oblateness and obliquity and the semimajor axes involved.

Equation 2 shows that the contribution from each satellite to q, the factor that is added to J_2, is proportional to the product of the mass of the satellite and the square of its distance from the planet. The contribution of Titan to the precession constant dominates the contribution from J_2, and this contribution increases as Titan migrates outward.

Resonance escape mechanisms

We next consider how the Saturn system could have escaped the resonance with Neptune. We identify two possibilities: First, the satellites' contribution to the precession of Saturn could have changed because of changes in their orbits (Eq. 2). This might have happened by the passage of the system through an orbital resonance involving the satellites. Second, the system could have escaped the Neptune resonance if a satellite was ejected from the system or collided with Saturn (removing a term in the sum in Eq. 2). A close encounter of a satellite with Saturn could have produced the debris that has evolved into the rings.

We investigated the first possibility through direct integration of the system using the full numerical model. We find that two principal orbital resonances are encountered (see supplementary text), which have been previously studied (*25*, *26*). We carried out integrations of the full system backward in time for ~200 Myr, with the Saturn moment of inertia that was determined with differential rotation and with various rates of tidal evolution that are consistent with the measured rate of evolution of Titan (*21*). These integrations confirm that the Saturn system is currently not in the Neptune resonance.

In no case did we find changes in the satellite orbits that were sufficiently large to allow the system to escape the Neptune resonance. Figure 2 shows an example numerical integration. The evolution coincides with the resonance model over the full span of the integration, indicating that passage through these orbital resonances cannot take the system out of the Neptune resonance. The comparison also illustrates that no other, previously unknown, strong orbital resonance was encountered.

Instability of an additional satellite

The second possibility is that there was previously an additional satellite in the Saturn system and that this satellite suffered some

orbital instability that led to either its escape or its collision with Saturn. With the loss of the hypothetical satellite, Chrysalis, the precession rate would have suddenly changed, allowing the system to escape the Neptune resonance. By requiring that the system evolved to the present configuration, we place constraints on when this could have occurred.

While in the Neptune resonance, the resonance angle σ oscillates about zero. Because σ does not change when a satellite is lost, Chrysalis could only have been lost when σ was close to zero in the simulations of the full system, backward in time from the present, without Chrysalis.

We have determined that the moment of inertia of Saturn is a little too small for the system to be in the Neptune resonance today, or the precession constant is a little too high. In the past, as Titan was closer to Saturn, the precession constant was smaller (Eq. 2). Therefore, there was a moment in the past when the system crossed the resonance. Figure 2 shows that this happens in the example simulation at about 100 Myr before present, where the motion of σ reverses direction. Figure 3 shows the evolution in terms of the precession constant. The loss of Chrysalis connects the evolution with Chrysalis to the evolution without Chrysalis. The system evolves into the resonance, then to higher obliquity as the precession constant changes because of the migration of Titan, at which point Chrysalis could have been lost, causing the precession constant to suddenly decrease. The subsequent evolution passes through the resonance to the currently observed Saturn system.

In this example simulation, the most recent time that Chrysalis could have been lost is about 160 Myr before present. In the full suite of simulations that vary the rate of tidal evolution of Titan, we find that the loss of Chrysalis could have occurred roughly 100 to 200 Myr before present. The combination of evolution in the Neptune resonance, followed by recent loss of Chrysalis, accounts for both the present-day obliquity of Saturn and the system's proximity to the Neptune resonance.

To explore the possibility that Chrysalis's orbit was destabilized, we integrated the full system with Chrysalis placed between Titan and Iapetus. As Titan migrates in the simulations, the Titan-Chrysalis pair encounters orbital resonances. We focused our exploration on the 3:1 mean-motion resonance (at which the orbital period of Chrysalis is approximately three times the orbital period of Titan), because this is the first strong resonance that would have been encountered as Titan migrated outward. The mass of Chrysalis must be chosen so that the precession constant has the required change. For the 3:1 resonance, the mass of Chrysalis must be approximately equal to the mass of Iapetus, though the value depends on when the 3:1 resonance is encountered, which in turn depends on the rate of tidal evolution of Titan. In these simulations, we set the tidal evolution rate for Titan to be 13.75 cm year^{-1} and the mass of Chrysalis to equal the mass of Iapetus. The initial conditions are taken from the backward simulation shown in Fig. 2.

We carried out integrations with Titan's orbital semimajor axis initially smaller than is required to be in the 3:1 resonance with Chrysalis. As Titan migrates outward, the system reaches the resonance, the behavior becomes chaotic, and the orbital eccentricity of Chrysalis rapidly increases, leading to close encounters with the other satellites (fig. S5).

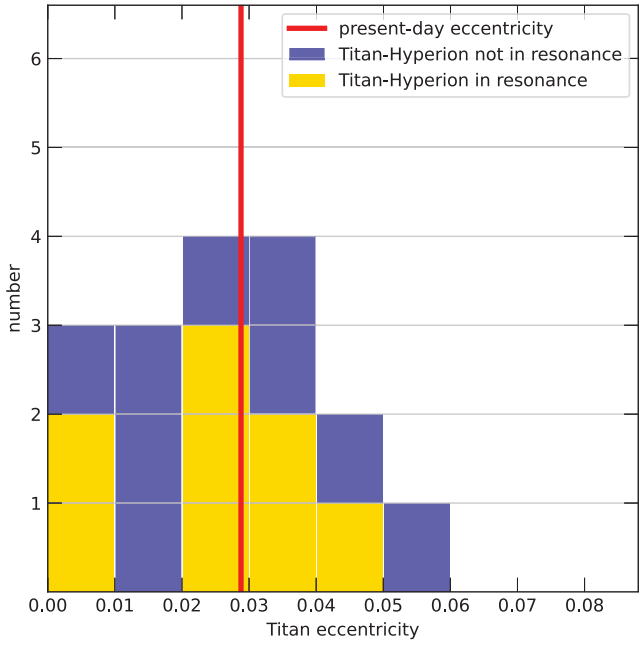

Fig. 5. Histogram of the eccentricity of Titan at the moment when Chrysalis experiences a grazing encounter with Saturn. Yellow (blue) bars indicate simulations in which Titan and Hyperion are (are not) left in a 4:3 mean motion resonance, in which we find Hyperion today. The vertical red line indicates the current eccentricity of Titan.

Exploration of an unstable system

We explored the expected outcomes of this scenario by simulating the system starting in the chaotic zone of the 3:1 Titan-Chrysalis resonance. We studied 390 cases, started with slightly different initial conditions (*21*). These integrations included Hyperion because Chrysalis repeatedly crosses its orbit. The present obliquity of Saturn could be explained if Chrysalis was either lost by ejection on a hyperbolic orbit or broken up during a grazing encounter with Saturn, with most of the material eventually hitting Saturn. In the latter case, a breakup of the satellite could explain the age of Saturn's rings.

The evolution of Chrysalis follows a typical pattern. In the first stage, the eccentricity and semimajor axis explore the chaotic zone and migrate to larger eccentricity. This stage is illustrated for an example simulation in Fig. 4A. This is followed by numerous close encounters with both Titan and Iapetus. The number of encounters varies but is typically of the order of a few tens. These encounters lead to an increase in the semimajor axis and eccentricity of Chrysalis. This stage is illustrated in Fig. 4B. Eventually, Chrysalis either has a close encounter with Saturn, is ejected from the satellite system, or has a collision with Titan, Hyperion, or Iapetus. For the simulation in Fig. 4, Chrysalis has a grazing encounter with Saturn at a distance of $1.9R_e$, close enough to undergo tidal disruption followed by formation of a ring (*27*).

Of our 390 simulations, there were 90 cases in which Hyperion was left with an orbit that was within $1.5R_e$ of its present orbit. Of these, there were 19 cases in which Chrysalis became hyperbolic (21%) and 17 Saturn grazers (18%) (the distance became smaller than $2.5R_e$ from Saturn; see supplementary text). Both of these cases would allow the system to escape the Neptune resonance (39%); those with Saturn grazers could make the rings. Hyperion's orbit is modified somewhat, so we cannot determine where it originated before Chrysalis was scattered. In 8 of the 17 grazing cases (47%), Hyperion was left librating in the Titan-Hyperion 4:3 mean motion resonance, as observed today (*28*).

The simulated Chrysalis has multiple encounters with Titan and Iapetus, so we expect that their orbits were modified. Titan's orbital eccentricity is of particular interest, because its relatively large value of 0.0288 has been considered a puzzle (*29*). In these integrations, we set the initial eccentricity of Titan to be zero; at the time of the encounter of Chrysalis with Saturn, we find that the eccentricity of Titan ranges from 0.004 to 0.055, with a mean of 0.026 and standard deviation of 0.015

(Fig. 5). The scattering of Chrysalis off of Titan leads to an orbital eccentricity of Titan similar to the current value.

We conclude that the loss of the hypothetical satellite Chrysalis can explain the obliquity of Saturn, the young age of its rings, and the eccentricity of Titan. The increased eccentricity and concomitant tidal heating (proportional to the square of the eccentricity) of Titan might also explain the presence of short-lived methane in its atmosphere (*30*).

Formation of Saturn's rings

A close encounter of Chrysalis with Saturn would have caused Chrysalis to break apart. If we assume that Chrysalis was predominantly made of water ice, like Iapetus, then this debris could have developed into Saturn's rings (*27*). Previous simulations of the formation of the rings from a disrupted cometary body, similar to the mass we assume for Chrysalis, indicate that it provides enough mass to produce the present-day rings (*31*).

The required timing of the loss of Chrysalis coincides with the estimated age of the rings. In our scenario, the ring age is anchored to a measured quantity, the rate of Titan's orbital expansion (*14*).

We propose that Saturn once had an additional satellite, Chrysalis; that the system was previously in the spin-orbit precession resonance with Neptune; that Saturn's obliquity increased as the precession rate changed because of the migration of Titan; that it escaped the precession resonance because of an instability of the orbit of Chrysalis; and that a close encounter of this hypothesized satellite with Saturn led to the formation of its rings.

REFERENCES AND NOTES

1. W. R. Ward, D. P. Hamilton, *Astrophys. J.* **128**, 2501–2509 (2004).
2. P. Goldreich, S. Tremaine, *Annu. Rev. Astron. Astrophys.* **20**, 249–283 (1982).
3. Z. Zhang *et al*., *Icarus* **294**, 14–42 (2017).
4. L. Iess *et al*., *Science* **364**, eaat2965 (2019).
5. A. Crida, S. Charnoz, H.-W. Hsu, L. Dones, *Nat. Astron.* **3**, 967–970 (2019).
6. A. W. Harris, W. R. Ward, *Annu. Rev. Earth Planet. Sci.* **10**, 61–108 (1982).
7. G. Cassini, *Traite de L'origine ede Progres de L'Astronomie* (Paris, 1693).
8. S. J. Peale, *Astron. J.* **74**, 483–489 (1969).
9. J. Laskar, P. Robutel, *Nature* **361**, 608–612 (1993).
10. J. Touma, J. Wisdom, *Science* **259**, 1294–1297 (1993).
11. W. R. Ward, *Science* **189**, 377–379 (1975).
12. M. Saillenfest, G. Lari, G. Boué, *Nat. Astron.* **5**, 345–349 (2021).
13. M. Saillenfest, G. Lari, G. Boué, A. Courtot, *Astron. Astrophys.* **647**, A92 (2021).
14. V. Lainey *et al*., *Nat. Astron.* **4**, 1053–1058 (2020).
15. G. F. Lindal, D. N. Sweetnam, V. R. Eshleman, *Astron. J.* **90**, 1136–1146 (1985).
16. B. Militzer, W. B. Hubbard, *Astrophys. J.* **774**, 148 (2013).
17. W. B. Hubbard, *Astrophys. J.* **768**, 43 (2013).
18. B. Militzer, S. Wahl, W. B. Hubbard, *Astrophys. J.* **879**, 78 (2019).
19. J. Wisdom, W. B. Hubbard, *Icarus* **267**, 315–322 (2016).
20. W. B. Hubbard, *Icarus* **137**, 357–359 (1999).
21. Materials and methods are provided in the supplementary materials.
22. S. Tremaine, *Icarus* **89**, 85–92 (1991).
23. R. Brasser, M. H. Lee, *Astron. J.* **150**, 157 (2015).
24. S. Tremaine, J. Touma, F. Namouni, *Astron. J.* **137**, 3706–3717 (2009).
25. W. Polycarpe *et al*., *Astron. Astrophys.* **619**, A133 (2018).
26. M. Ćuk, L. Dones, D. Nesvorný, K. J. Walsh, *Mon. Not. R. Astron. Soc.* **481**, 5411–5421 (2018).
27. L. Dones, *Icarus* **92**, 194–203 (1991).
28. A. T. Sinclair, *Mon. Not. R. Astron. Soc.* **160**, 169–187 (1972).
29. C. Sagan, S. F. Dermott, *Nature* **300**, 731–733 (1982).
30. G. Tobie, J. I. Lunine, C. Sotin, *Nature* **440**, 61–64 (2006).
31. R. Hyodo, S. Charnoz, K. Ohtsuki, H. Genda, *Icarus* **282**, 195–213 (2017).
32. J. Wisdom *et al*., SaturnObliquityRings, Harvard Dataverse Repository (2022); https://doi.org/10.7910/DVN/RJZXGW.
33. J. Wisdom, NbodySatellites, Zenodo (2022); https://doi.org/10.5281/zenodo.6960630.

ACKNOWLEDGMENTS

We thank J. Touma, S. Tremaine, and T. Perron for carefully reading the manuscript. C. Hill provided computing time on the MIT Engaging Cluster. **Funding:** Support for this work was provided by NASA's SSW program (J.W., F.N., and R.D.), NASA's extended Juno mission (W.B.H. and B.M.), the National Nuclear Security Administration (B.M.), NASA's CDAP program (R.G.F.), and the NSF Graduate Research Fellowships Program (B.D.). **Author contributions:** J.W. and F.N. designed the overall research; J.W. noticed that Titan's migration could lead to capture in the Neptune resonance; B.M., W.B.H., and J.W. developed interior models; J.W. wrote the satellite evolution software; R.D. developed the resonance model; J.W. suggested that an extra satellite might have been resonantly destabilized and form the rings; R.D. identified the conditions for escape; and J.W. and R.D. carried out the simulations and analysis. F.N. and B.G.D. provided input throughout. R.G.F. validated the numerical model of Saturn's pole. **Competing interests:** The authors declare no competing interests. **Data and materials availability:** All data and software have been deposited in Harvard Dataverse (*32*). The satellite evolution code is also available on Zenodo (*33*).

SUPPLEMENTARY MATERIALS

science.org/doi/10.1126/science.abn1234
Materials and Methods
Supplementary Text
Figs. S1 to S5
Table S1
References (*34*–*51*)

Submitted 4 November 2021; accepted 12 August 2022
10.1126/science.abn1234